Available online at www.sciencedirect.com
ScienceDirect
Journal of the European Ceramic Society 30 (2010) 2497–2504
www.elsevier.com/locate/jeurceramsoc

Anomalous increase in specific volume upon crystallization of some alloys in the zirconia–yttria–erbia system

A.A. Frolov [a,*], Yu.A. Frolov [b], E.R. Andrievskaya [a]

[a] *I.N. Frantsevich Institute for Problems of Materials Science, NAS of Ukraine, Kiev 03142, Ukraine*
[b] *Institute of Magnetism, NAS of Ukraine, 36-b, Vernadsky Blvd., Kiev 03142, Ukraine*

Received 11 June 2009; received in revised form 9 March 2010; accepted 2 April 2010
Available online 15 May 2010

Abstract

New inorganic materials with dominant ionic chemical bonds which expand upon crystallization at room temperature have been discovered. This effect has been observed in alloys of the ZrO_2–Y_2O_3–Er_2O_3 system. It can be interpreted as transition existence from crystal structure with dominant ionic bonds to the one with dominant covalent or covalent-metallic bonds while heating below the melt point. So the phase transition from cubic C phase to hexagonal H which occurs in these materials at about 2300 °C should be linked to changing in the dominant type of chemical bonds.

Such a phenomenon should be take place upon oxides crystallization of rare-earth elements which have physicochemical properties and electron structure similar to those of Y_2O_3, namely of heavy lanthanides oxides Ho_2O_3, Tm_2O_3, and Yb_2O_3; upon the crystallization of their alloys with each other and with Er_2O_3 and Y_2O_3.

Keywords: Thermal properties; Y_2O_3; ZrO_2; Rare earth oxides; Refractories

1. Introduction

REE oxides and their alloys among each other and with Zr oxide are widely used as the materials having high melting temperature, thermodynamic stability, strength and crack resistance and can be used in developing of special-purpose refractories, fuel elements, etc. These alloys have a lot of phase transitions at high temperatures. It has been found out that some of the alloys have anomalous specific volume changing (expansion) upon crystallization.[1,2] Consequently, these materials are of great interest for research and practical application.

Inorganic materials which expand upon crystallization cannot be frequently observed. Undoubtedly, the first known substance of this type is water, in the point of the phase transition of "water–ice". Similar behaviour was also found for Bi and Sb already in the 19th century.[3]

The value of volume increase upon crystallization ($\Delta V/V_s$) is determined by the formula:

$$\frac{\Delta V}{V_{sol}} \times 100(\%) = \frac{(V_{sol} - V_{liq})}{V_{sol}} \times 100(\%) \quad (1)$$

where V_{sol} and V_{liq} are specific volumes of solid phase and liquid phase (g/cm^3), respectively. Most of the currently known inorganic substances expanding upon crystallization are (in parenthesis $(\Delta V/V_{sol}) \times 100(\%)$ is indicated): (1) chemical compounds with chemical bonds of the hydrogen type: H_2O (8.3%)[4,5]; (2) elementary semiconductors: Si (10.0%,[6,7] 8.4%,[8] 5.4%[9]) and Ge(5.7%,[6,8] 4.75%[7]); (3) metallic Ga (3.24%,[6] 3.2%[10,11]); (4) semimetals: Sb (0.95%[6]), Bi (3.3%[6]), and some of their alloys; (5) semiconductor compounds $A^{III}B^{V}$: GaSb (9.6%,[6] 8.2%[7]), InSb (12.5%[6,7]), AlSb (12.9%[6,7]), GaAs (10.7%[6,7]), and InAs (7.1%[6,7]); (6) semiconductor compounds Mg_2B^{IV}: Mg_2Si (23.3%[7]), Mg_2Sn (2.5%[6], 2.03%[7]), and Mg_2Pb (2.03%,[6] 4%[7]); (7) plutonium and some of its alloys,[12] and (8) some compositions of grey irons.[13] The volume increase of grey cast iron at the eutectic temperature is related to the growth of graphite grains. The latter have a larger specific volume than that of the dissolved carbon.[13] The anomalous behaviour of water upon crystallization is connected with the presence of

* Corresponding author. Tel.: +380 44 393 0974; fax: +380 44 424 2131.
E-mail address: Al-frolov@yandex.ru (A.A. Frolov).

0955-2219/$ – see front matter © 2010 Elsevier Ltd. All rights reserved.
doi:10.1016/j.jeurceramsoc.2010.04.003

directional hydrogen bonds between water molecules. Under freezing, water molecules are arrayed into a lattice according to the directions of chemical bonds, which leads to the formation of a "loose" ice structure, and therefore to the increase of the specific volume.[4,5] Semiconductors Si and Ge[9] are typical materials with dominant covalent bonds. Large amount of directional covalent bonds is observed in the crystals of semimetals Sb, Bi,[6] metallic Ga[10,11] and semiconductor compounds GaSb, GaAs, InSb, InAs, AlSb, Mg_2Si, Mg_2Sn, and Mg_2Pb as well.[7] The processes of melting and crystallization of these materials have been reviewed.[7,10,11] The large covalent component of chemical bonds acts in plutonium and its alloys.[12,14] Tanaka,[15] analyzing *P–T* diagrams, has made the conclusion that the effect of expansion upon crystallization of Si, Ge, Sb, Bi, Ga, and InSb is the consequence of the directional covalent bonds existence.

Thus, in all the substances with a positive volume effect of crystallization, we can observe directional chemical bonds domination. They can form a "loose" lattice of substance upon crystallization. Therefore, the availability of a large component of the directional chemical bonds is a necessary but certainly insufficient condition of expansion upon crystallization.

The above list of substances shows that the positive volume effect of crystallization is not observed in substances with dominant ionic bonds. Though, an anomalous shape of ingot surface formation has been found upon crystallization of the refractory zirconia–yttria–erbia system in the centrosymmetrical temperature field.[1,2] These alloys are materials with dominant ionic bonds and so are not expected to be expanded upon freezing. But the formation of anomalous shape of ingot surface can be related to expansion upon crystallization. The positive volume effect of crystallization in the alloys which included ZrO_2 was related to the emergence of point defect complexes in the course of a hexagonal structure formation in solutions of nonisovalent metals oxides (zirconium and rare-earth elements). However, the following experiments have shown that the positive values of the volume crystallization effect are typical for pure Y_2O_3 and the binary Y_2O_3–Er_2O_3 alloys, where ZrO_2 is absent. Therefore, the aim of this work was to find out the reason of the anomalous behaviour of the Y_2O_3–Er_2O_3 alloys upon crystallization.

In this research, fused ingots of zirconia–yttria–erbia alloys of various compositions have been obtained. All of these oxides are substances with dominant ionic bonds. It is significant for discussion of high temperature properties of such alloys.

The values of the chemical bond ionicity of the tested oxides were estimated by using the Pauling formula[16]:

$$P\% = 1 - \exp\left[-0.25(X_A - X_B)^2\right] \quad (2)$$

where $(X_A - X_B)$ is the electronegativity difference for A and B atoms.

We used the following parameters of electronegativity: $X_{Zr} = 1.4$[16]; $X_{Er} = 1.2$ (1.25)[17]; $X_Y = 1.3$[17]; and $X_O = 3.5$.[16] Chemical bond ionicity (I %) of considered oxides were obtained: $I(ZrO_2) = 67\%$; $I(Er_2O_3) = 73\%$; $I(Y_2O_3) = 70\%$.

For comparison, the chemical bond ionicity of NaCl is 67%.[16] Thus the ionicity of ZrO_2, Er_2O_3, and Y_2O_3 are equal to or higher than that of such a typical ionic compound as NaCl.

2. Experimental procedure

It is well known that the phenomenon of volume changing in transition from liquid to solid state causes mass transfer in the processes of directional crystallization and zone cleaning.[18] The specific volume of such widespread semiconductors as Si and Ge increases upon crystallization. So the mass of these melts is partially transferred along the line of melting zone movement. It is well known in metallurgy that shrink cone formation occurs in most substances under crystallization of melted material in a centrosymmetrical temperature field from the walls of the crucible to its center. During the directional crystallization of substances which have positive volume effect of crystallization, for example Ge, along the lines from the edge to the center of the melting zone, the formation of a salient cone on the ingot surfaces occurs.[19]

Alloy ingots of the ZrO_2–Y_2O_3–Er_2O_3 system were obtained by the melting method in the focal zone of the optical furnace.[2,20,21]

In the focal zone center of this optical furnace, the energy flow density can reach value of $E_{max} = 1.6 \times 10^4$ kWt/m^2, which allows melting the most refractory oxide materials. In order to improve the temperature field radial symmetry, a sample (20 mm in diameter) was rotated under heating and cooling. The gradual crystallization of material from the melt pool edge to the center was induced by decreasing the energy light flow density in order to obtain the necessary conditions for crystallization. No special safe temperature conditions for slow cooling and annealing after solidification were used. Samples were cooled in air. The crystallization process of the ternary ZrO_2–Y_2O_3–Er_2O_3 system alloys was put onto video.

All obtained ingots had inner volume defects (pores, cracks, hollow spaces). Their maximal concentration was in the center of ingots. Therefore, the samples for the porosity measurements were cut out from the central zones of the Y_2O_3 ingots. The porosity was measured by using the method of hydrostatic weighing with preliminary samples vacuum treatment.[22] The weighing accuracy was up to 0.0001 g and the weighing error did not exceed 0.5–1%.

3. Results

The following characteristic changes were observed in the crystallized ingots: (1) shrink cone formation occurred on the ingot surfaces of the 100% ZrO_2 and most of the tested samples during of the processes crystallization in the focal zone of the optical furnace (Fig. 1); (2) horizontal plane was formed on the ingot surface with 100% Er_2O_3 composition (Fig. 2) (if the melt pool surface had convex geometry, it did not change); (3) salient cones were formed on the ingot surfaces with large concentration of erbia and yttria (Fig. 2); (4) some of the alloy ingots with intermediate concentrations of zirconia were broken in the explosion-like manner after being crystallized (Fig. 3); (5) some of the alloy ingots with intermediate concentrations of zirconia (more than in (4)) were broken under cooling.

The crystallization processes in the binary ZrO_2–Er_2O_3 and ZrO_2–Y_2O_3 alloys have been studied before.[2] In that case

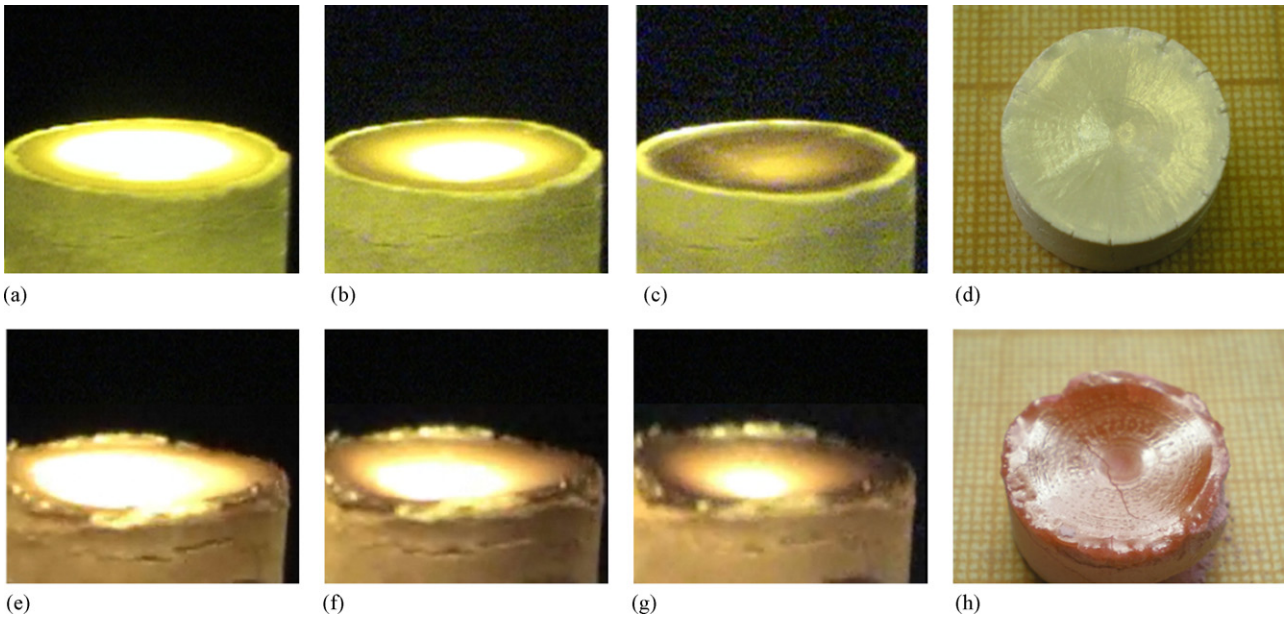

Fig. 1. Stages of shrink cone formation in condition of centrosymmetrical temperature field: (a), (b), (c) stages of shrink cone formation; (d) shrink cone on the sample surface of 100% ZrO_2 and (e), (f), (g) stages of shrink cone formation, (h) shrink cone on the sample ingot surface of alloy of composition 50% ZrO_2–50% Er_2O_3.

salient cone formation on hypoeutectic alloys ingot surfaces takes place. Hypereutectic alloys in the concentration area of the hexagonal phase existence break in the explosion-like manner. The concentration areas classification for alloys in the ternary ZrO_2–Y_2O_3–Er_2O_3 system according to the ingot surfaces crystallization behaviour and shape is shown in Fig. 4.

The studied system is characterized by the following features:

(1) Salient cones are formed on the ingot surfaces in the alloy compositions having hexagonal H phase primary crystallization such as alloys of the binary Er_2O_3–Y_2O_3 system, 100% Y_2O_3, and alloys with small ZrO_2 concentration. The surface ingot shapes with 100% Er_2O_3 do not change. These are areas *I* and *II*.

(2) The alloys with high ZrO_2 concentration are situated in the area of the C phase primary crystallization and the following $\langle C\rangle \rightarrow \langle C\rangle + \langle H\rangle$ transition under cooling (area *III*). In his case a shrink cone starts its formation and the sample explosion-like break occurs.

(3) The alloys with higher ZrO_2 concentration are located outside the area of incongruent transitions crystallize with a shrink cone formation (areas *IV*, *V*, and *VI*). But some of the alloy ingots with intermediate concentrations become broken under the subsequent cooling (area *VII*). This process is possible but not compulsory.

The most interesting result of such observations is the formation of the salient cone on the ingot surface of the Y_2O_3 and some alloy compositions. The initial melt pool and solidified ingot of

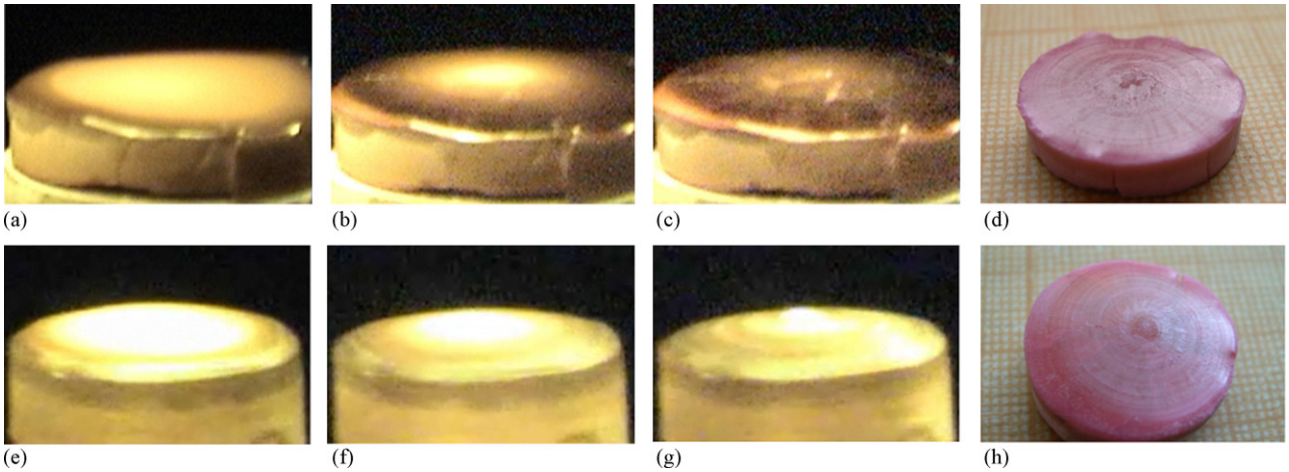

Fig. 2. Stages of "anomalous" ingot surface formation in condition of centrosymmetrical temperature field: (a), (b), (c) stages of plane surface formation, (d) the sample surface of 100% Er_2O_3 and (e), (f), (g) stages of salient cone formation, (h) the sample surface of 10% ZrO_2–90% Er_2O_3 alloy.

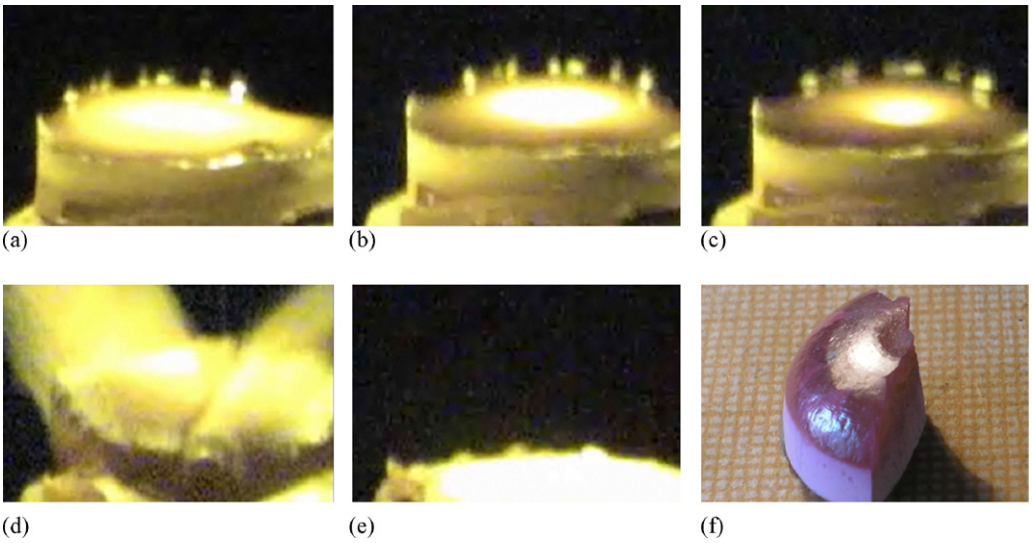

Fig. 3. Stages of ingot crystallization of the alloy with 25% ZrO_2–75% Er_2O_3 composition: (a) melt pool; (b) intermediate stage of solidification; (c) start of shrink cone formation; (d) stage of explosion-like breaking; (e) residual part of pressed sample after the melted ingot top and sintered part being "exploded"; (f) fragment of broken ingot with a part of shrink cone.

Y_2O_3 are shown in Fig. 5a, b. The schematic drawing of the volume change estimation upon crystallization is illustrated in Fig. 5c, d. The method of solid-to-liquid specific volumes ratio rough estimation via analysis of ingot surface shape has been developed.[23,24] But, the mentioned method uses an "assumed" shape of the melt pool surface. In this paper, we propose to estimate changing of true specific volume $((\Delta V/V)_{true})$ with the use of the melt pool and ingot side views at axial symmetry approximation.[22] According to (1)

$$\left(\frac{\Delta V}{V}\right)_{true} = \frac{(V_{sol} - V_{liq})}{V_{sol}} \tag{1a}$$

The method has three general sources of errors. Such as:

(1.1) The shapes of melt pool and ingot are not absolutely symmetrical. Fig. 5.

The volume of liquid phase (V_{liq}) and ingot (V_{ing}) can be determined as the volumes of corresponding rotary figures multiplied by a certain perspective distorting coefficient (k).

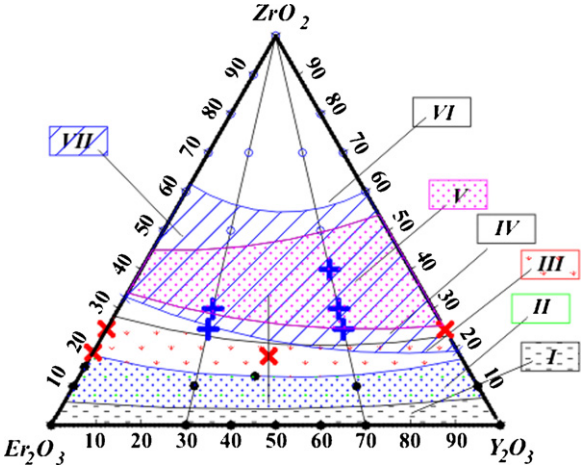

Fig. 4. Crystallization behaviour of alloys of the ZrO_2–Y_2O_3–Er_2O_3 system in centrosymmetrical temperature field: (*I*) concentration area of the H phase primary crystallization and the following ⟨H⟩ → ⟨C⟩ transition upon cooling; (*II*) area of the H phase primary crystallization and the following ⟨H⟩ → ⟨H⟩ + ⟨C⟩ → ⟨C⟩ transitions; (*III*) area of the C phase primary crystallization and the following ⟨C⟩ → ⟨C⟩ + ⟨H⟩ → ⟨C⟩ transitions; (*IV*) area of the C phase crystallization and the following secondary crystallization ⟨C⟩ → ⟨C⟩ + ⟨F⟩; (*V*) area of the F phase primary crystallization and the following ⟨F⟩ → ⟨C⟩ + ⟨F⟩ transition; (*VI*) area of the F phase crystallization; and (*VII*) expected area which corresponds to the eutectoidal reaction of the formation of chemical compounds with larger specific volume than that of the solid matrix at lower temperature. Spot symbols correspond to: (◯) shrink cone formation; (×) explosion-like break of sample; (†) sample break upon following cooling; (●) formation of a salient cone or lack of surface shape change (100% Er_2O_3).

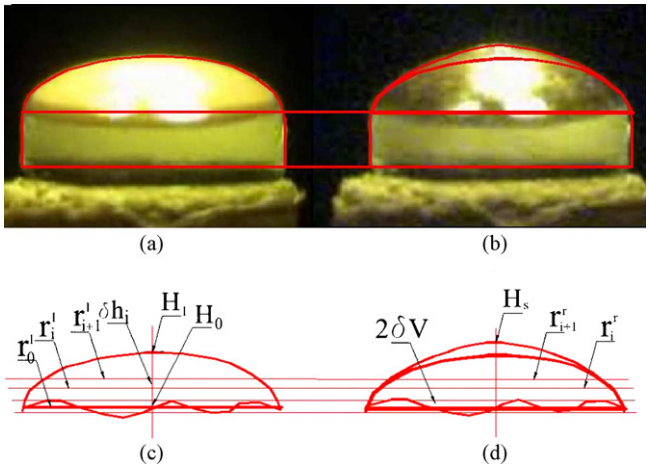

Fig. 5. Side projections of Y_2O_3 sample and design diagram for: (a) side projection of the melt pool before crystallization; (b) side projection of the ingot; (c) design diagram of melt pool; (d) design diagram of ingot. r_0^l, r_i^l, r_{i+1}^l are radii of based (0), ith and $i+1$th truncated cones that were re-established with left part of side projection, conformably. r_i^r, r_{i+1}^r are radii of ith and $i+1$th truncated cones that were re-established with right part of side projection, conformably. H_0, H_l, H_s are ordinates of bottom pool melt (ingot), top of pool melt, top of ingot conformably. $2\delta V$ is the volume of the bottom ingot layer.

This inaccuracy can be taken into account in the following way:

The volumes of the melt pool (V_{liq}) and apparent volume of ingot (V_{ing}) can be calculated as average value of the rotary figures (of the left (V^l_{mel}, V^l_{ing}) and right (V^r_{mel}, V^r_{ing}) parts of corresponding images) multiplied by distorting coefficient k:

$$V_{liq} = k\frac{V^l_{mel} + V^r_{mel}}{2} \quad \text{and} \quad V_{ing} = k\frac{V^l_{ing} + V^r_{ing}}{2} \tag{3}$$

where V^l_{mel}, V^r_{mel}, V^l_{ing}, V^r_{ing} are equal to the sums of the volumes of the elementary truncated cones,

$$V^l_{mel} = \frac{\pi}{3}\left\{\sum_{H_i=H_0}^{H_i=H_l} \delta h_i \cdot \left[\left(r^l_i\right)^2 + \left(r^l_{i+1}\right)^2 + r^l_i \cdot r^l_{i+1}\right]\right\} \tag{4a}$$

$$V^r_{mel} = \frac{\pi}{3}\left\{\sum_{H_i=H_0}^{H_i=H_l} \delta h_i \cdot \left[\left(r^r_i\right)^2 + \left(r^r_{i+1}\right)^2 + r^r_i \cdot r^r_{i+1}\right]\right\} \tag{4b}$$

Similarly:

$$V^l_{ing} = \frac{\pi}{3}\left\{\sum_{H_i=H_0}^{H_i=H_s} \delta h_i \cdot \left[\left(r^l_i\right)^2 + \left(r^l_{i+1}\right)^2 + r^l_i \cdot r^l_{i+1}\right]\right\} \tag{4c}$$

$$V^r_{ing} = \frac{\pi}{3}\left\{\sum_{H_i=H_0}^{H_i=H_s} \delta h_i \cdot \left[\left(r^r_i\right)^2 + \left(r^r_{i+1}\right)^2 + r^r_i \cdot r^r_{i+1}\right]\right\} \tag{4d}$$

where H_i is identification code of the ith elementary truncated cone; H_0 is the ordinate of the bottom of the melt pool and solid ingot of Y_2O_3; H_m is the ordinate of the top of the Y_2O_3 melt pool; H_s is the ordinate of the top of the Y_2O_3 ingot; δh_i is the height of the ith elementary truncated cone. r^l_i and r^l_{i+1} are left base radii of the ith elementary truncated cone in the side views. r^r_i and r^r_{i+1} are right base radii of the ith elementary truncated cone in the side views.

To make the images clear, the right dimensions of the melt pool diagram and the left ones of the ingot diagram are not shown in Fig. 5c, d.

As we estimate the true changing of specific volume $(\Delta V/V_{ing})_{true}$, it can be written as follows:

$$\left(\frac{\Delta V}{V_{ing}}\right)_{true} = \frac{k}{k}\frac{(V_{ing} - V_{liq})}{V_{ing}} \tag{5}$$

Coefficient k is cancelled (it is a value of volume distortion for the side views interpretation), and so we have that $(\Delta V/V_{ing})_{true}$ does not depend on distortion at the side views interpretation.

It should be emphasized that Fig. 5c, d. is the calculation scheme only, as even the outline thickness causes an appreciable error. Therefore, in practice we did it in the following way: the images of melt pool and ingot were printed in the same scale. Then the outline of the melt pool image was cut and placed on the ingot image. After that the elementary truncated cones were chosen in the images of the melt pool and ingot. By the method described above the estimation of apparent specific volume changing $(\Delta V/V_{ing})_{app}$ is:

$$\left(\frac{\Delta V}{V_{ing}}\right)_{app} = \left[0.067 \pm \delta_\Sigma\left(\frac{\Delta V}{V_{ing}}\right)\right] \tag{6}$$

where

$$\delta_\Sigma\left(\frac{\Delta V}{V_{ing}}\right) = \sqrt{\left[\delta_{sys}\left(\frac{\Delta V}{V_{ing}}\right)\right]^2 + \left[3\delta^{0.68}_{acc}\left(\frac{\Delta V}{V_{ing}}\right)\right]^2} \tag{7}$$

is the sum of $(\Delta V/V_{ing})_{app}$ estimation errors: the accidental standard error (squared error) multiplied by 3 ($3 \cdot \delta^{0.68}_{acc}(\Delta V/V_{ing})$, the confidence probability of such estimation equal 0.997) and systematic error ($\delta_{sys}(\Delta V/V_{ing})$). We have got in our experiments, that

$$3 \cdot \delta^{0.68}_{acc}\left(\frac{\Delta V}{V_{ing}}\right) = 0.024 \tag{8}$$

(1.2) The general systematic error ($\delta_{sys}(\Delta V/V_{ing})$) is caused by the fact that boundary surface between the ceramic base and melt pool (or fused solid phase) is not plane and cannot be determined exactly. Therefore the volumes of the melt pool and ingot are determined with the similar absolute systematic inaccuracy δV. δV can be defined as 1/2 volume of the rotated figure between lower planes in Fig. 5c, d. Accordingly, $(\Delta V/V_{ing})_{app}$ has systematic error of estimation. Investigations of fused ingot crosses showed that such systematic error ($\delta_{sys}(\Delta V/V_{ing})$) is no more than 0.1 or 0.2, as compared with relate changing of volume, and the limit value of such error in our experiments is:

$$\delta_{sys}\left(\frac{\Delta V}{V_{ing}}\right) \approx 0.2 \cdot \left(\frac{\Delta V}{V_{ing}}\right) \approx 0.0134 \tag{9}$$

According to (7), (8), (9), we have got for our experiments, that

$$\left(\frac{\Delta V}{V_{ing}}\right)_{app} \approx 0.067 \pm 0.027 \tag{10}$$

confidence probability equals to 0.997.

(1.3) Pores, cracks and other hollows increase apparent volume of the ingots. (Further, no hollows (bubbles) are considered to be in the melt of Y_2O_3). The true volume of solid phase (V_{sol}) is:

$$V_{sol} = V_{ing} - V_{por} \tag{11}$$

where V_{por} is total volume of porous, cracks and other volume defects in the ingot.

Porosity has been experimentally determined by the method of hydrostatic weighing in the distilled water with preliminary sample vacuum treatment. The obtained results showed that there was no open porosity in the fused samples. The closed porosity was[22]:

$$P = 2\text{–}2.5\% \tag{12}$$

If the estimation error of the volume changing has maximal negative value (−0.027) and the porosity of Y_2O_3 ingots has maximum possible value (according to (12) $P_{max} = 2.5\%$) then:

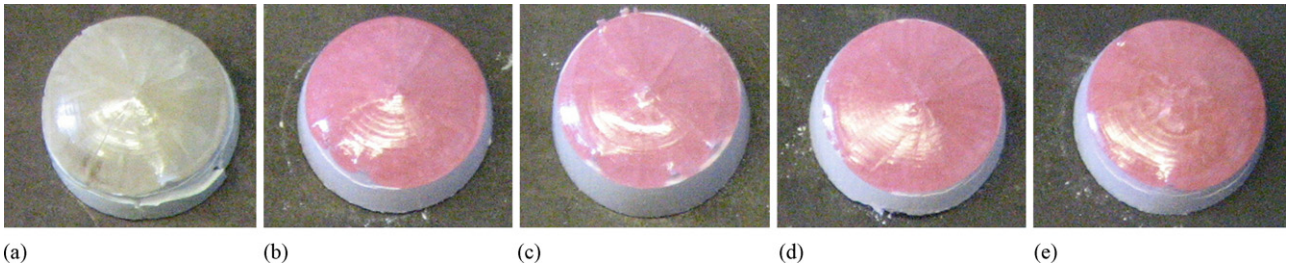

Fig. 6. General forms of ingot surface shapes of the boundary binary Er_2O_3–Y_2O_3 system alloys for the compositions: (a) 100% Y_2O_3; (b) 30% Er_2O_3–70%; (c) 40% Er_2O_3–60% Y_2O_3; (d) 60% Er_2O_3–40% Y_2O_3; (e) 70% Er_2O_3–30% Y_2O_3 (g).

$(\Delta V/V_{ing})_{app}$ equals, no less than 0.04 and thus, the true specific volume change of Y_2O_3 upon crystallization is no less than:

$$\left(\frac{\Delta V}{V_{ing}}\right)_{true} \times 100\% = \left[\left(\frac{\Delta V}{V_{ing}}\right)_{app} - P_{\max}\right] \times 100\% \approx 1.5\% \quad (13)$$

It is the smallest Y_2O_3 specific volume increase value upon crystallization that can be accepted according to our experiments.

So, the processes have observed in our experiments show that Y_2O_3 specific volume increases upon crystallization as well as in some alloys of the ZrO_2–Y_2O_3–Er_2O_3 system.

4. Discussion

The main unusual result obtained is the increase in the specific volume of some alloys of the ZrO_2–Y_2O_3–Er_2O_3 system upon the phase transition from liquid to solid phase. Possible causes of the expansion upon crystallization are the following: (1) a great number of macro- and microdefects such as pores, cracks, bubbles and other hollow spaces, which lead to increase of an apparent ingot volume, (2) formation of chemically induced vacancies in the metal sublattice created thanks to addition of larger valence metal oxides, and (3) the smaller density of the crystal phase compared to that of the melt, which occurs for substances with directional chemical bonds (as mentioned in Section 1).

The general forms of binary Er_2O_3–Y_2O_3 system ingot surfaces[25] are shown in Fig. 6.

The form of the ingot surface of 100% Er_2O_3 is shown in Fig. 2d.

The domination of directional chemical bonds in substances is a requirement for the "loose" crystal structure formation and expansion upon crystallization, as mentioned in the introduction. Therefore we can state that the hexagonal H phase forming upon the phase liquid–solid transition in alloys of the Er_2O_3–Y_2O_3 system represents a structure with dominant directional chemical bonds. The possible bonds for the materials studied can be covalent or covalent-metallic. It is well-known that under heating yttria and erbia have the phase transition from the cubic C to hexagonal H phase at about 2300 °C accompanied by volume increase,[26] which can be related to the transition to the dominant directional chemical bonds. Naturally, the reverse transition under cooling must be connected to rebuilding of the lattice to a structure with dominant ionic bonds typical for the C phase.

The nature of chemical bonds as is known depends on temperature and pressure. For example, the bond ionicity of such a traditional ionic compound as NaCl decreases with temperature increase.[27] It is evident that the ionic component of chemical bonds in the tested alloys decreases under heating too, and at certain temperature the directional component (covalent or

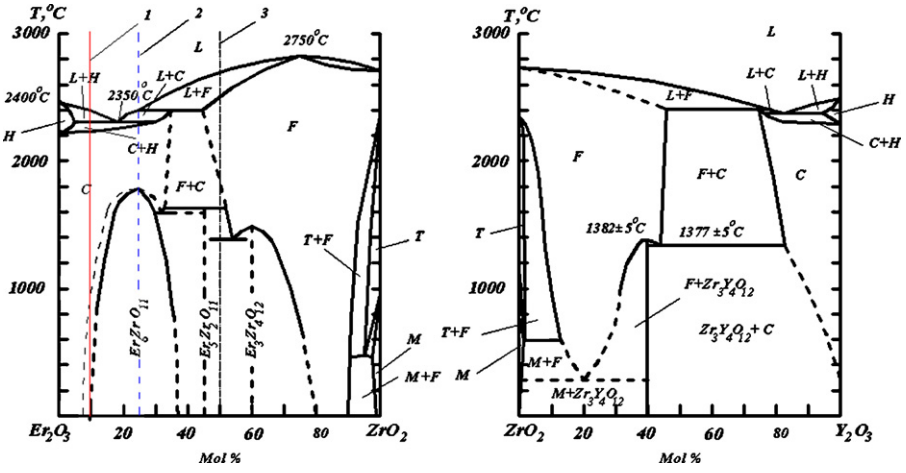

Fig. 7. Phase diagrams of the boundary binary systems: (a) Er_2O_3–ZrO_2[28,29]; (b) ZrO_2–Y_2O_3.[30] Compositions (1) 90% Er_2O_3–10% ZrO_2; (2) 80% Er_2O_3–20% ZrO_2; (3) 50% Er_2O_3–50% ZrO_2.

covalent-metallic) of the chemical bond becomes dominating to such a great extent that causes rebuilding of the lattice into a structure corresponding to the space direction of this bond component. In a particular case, such structures can have density lower than that of the disordered (molten) substance. Herein the specific volume has to increase with formation of long range ordering. This case is realized in some of the studied alloys.

It is reasonable to discuss the model of expansion upon crystallization due to "Directional chemical bonds formation" in parallel with the model based on the "Emergence of point defect complexes".[2]

The phase diagrams of the boundary binary Er_2O_3–ZrO_2[28,29] and ZrO_2–Y_2O_3[30] systems are shown in Fig. 7.

When the hypoeutectic melts of the boundary systems are cooling, the primary crystallization of the H phase occurs. The specific volume of such alloys increases upon crystallization. The replacement of Y^{3+}(Er^{3+}) by Zr^{4+} occurs in the formation of the H phases of the Er_2O_3–ZrO_2 and ZrO_2–Y_2O_3 alloys. In this case, the requirement for crystal electric neutrality leads to the appearance of additional vacancies in the metal sublattice. The replacement of every six Er^{3+} (Y^{3+}) ions by Zr^{4+} ions in the H phase lattice leads to the appearance of two additional vacancies in the metal sublattice and that is to the appearance of numerous additional vacancies in the volume of alloys.[2,20] Therefore, the specific volume of H phases in the ZrO_2–Er_2O_3, ZrO_2–Y_2O_3 and ZrO_2–Y_2O_3–Er_2O_3 alloys is greater than that in both 100% Er_2O_3, 100% Y_2O_3, and the corresponding intermediate Y_2O_3–Er_2O_3 alloys. The effect of specific volume increase upon crystallization of these alloys with a small additions of ZrO_2 is greater than that of pure oxides or their alloys. There is a salient cone on their surface and its size is larger than that of 100% Er_2O_3, 100% Y_2O_3 or the intermediate Y_2O_3–Er_2O_3 alloys. These alloys have composition (1) in Fig. 7a and composition of areas I and II in Fig. 4. It should be emphasized that we can see the value of specific volume increase upon crystallization related namely to the emergence of point defect complexes if a small quantity of ZrO_2 is added into 100% Er_2O_3, because the expansion upon pure Er_2O_3 crystallization is equal to zero. The plane ingot surface of 100% Er_2O_3 is shown in Fig. 2c, d. Similar effects for the ZrO_2–Y_2O_3–Er_2O_3 and ZrO_2–Y_2O_3 alloys are not so obvious and visible as for ZrO_2–Er_2O_3 ones.

The specific volume of the H phase is larger than that of the C phase. In the area of the secondary H phase crystallization, the latter is crystallized inside the C phase matrix for the second time. At first, shrink cones begin their formation on the surfaces of ingots and then the ingots brake into pieces. These alloys have composition (2) (Fig. 7a) and the composition of area *III* (Fig. 4). The shrink cones formed on the ingot surfaces of these alloys confirm the fact that the specific volume of the C phase is lower than that of the melt.

Under cooling of the alloys with high ZrO_2 concentration, the C phase primarily crystallizes in area *IV* with the following secondary crystallization transition $\langle C\rangle \rightarrow \langle C\rangle + \langle F\rangle$. The F phase primarily crystallizes in area *V* with the secondary crystallization transition $\langle F\rangle \rightarrow \langle C\rangle + \langle F\rangle$ and in area *VI*. The specific volumes of the C and F phases are lower than those of their melts, and shrink cones form on the surfaces of their ingots. The composition (3) (Fig. 7a) and the compositions of areas *IV*, *V*, and *VI* (Fig. 4) are related to these alloys.

The eutectoidal reactions $\langle F\rangle \rightarrow \langle F\rangle + \delta$ (δ') or $\langle F\rangle + \langle C\rangle \rightarrow \langle F\rangle + \delta$ (δ') exist in the ZrO_2–Y_2O_3–Er_2O_3 system in area *VII* at lower temperatures. Intermediate phases correspond to the chemical compounds $Zr_3Y_4(Er_4)O_{12}$ (δ phase) or $Zr_2Er_5O_{11}$ (δ' phase) for the boundary binary Er_2O_3–ZrO_2 and ZrO_2–Y_2O_3 systems (Fig. 7). The specific volumes of δ or δ' phases are larger than that of the F phase, and the alloy samples may be broken under rapid cooling (it is possible but not obligatory).

Therefore, the results of these experiments allow to state that the directional type of chemical bonds dominate in the described alloys in the area of the existence of high temperature hexagonal H phase, and the $\langle C\rangle \rightarrow \langle H\rangle$ phase transition under heating is accompanied with changing of the chemical bond type from dominant ionic one to dominant covalent or covalent-metallic. In the last case, the phase transition may be accompanied by the changing of the conductivity type from dielectric (semiconducting) to metallic.

It is possible that phase transitions of the $\langle C\rangle \rightleftarrows \langle H\rangle$ type existing in other rare earth metal oxides and their alloys are similar to the ones in the ZrO_2–Y_2O_3–Er_2O_3 system. Therefore, the change in the chemical bond type from the dominant ionic bond to dominant covalent or covalent-metallic one is the reason for such transitions too. Nevertheless, these alloys should not inescapably expanding upon crystallization because, in some way it is an extreme case. The phenomenon of specific volume conservation was found upon crystallization of rare earth metal oxides having physicochemical properties and electron structure similar to those of Y_2O_3. Such substances are the heavy lanthanides Ho_2O_3, Tm_2O_3, and Yb_2O_3 oxides.[22] It is possible that the alloys of the above mentioned oxides with each other and with Er_2O_3 and Y_2O_3 can have the similar properties. The addition of ZrO_2 or HfO_2 into such substances in the concentration area of the H phase primary crystallization leads to an additional volume increase due to the appearance of chemically induced vacancies in the metal sublattice.

5. Conclusions

The phenomenon of the specific volume increase upon crystallization of some alloys of the ZrO_2–Y_2O_3–Er_2O_3 system has been discovered. These alloys are compounds with dominant ionic chemical bonds under normal conditions, whereas expansion upon crystallization is a feature of substances with the directional type of chemical bonds. Therefore, the phase transition of the cubic C phase to hexagonal H phase accompanied by volume increase, which exists in some alloys of the investigated system at about 2300 °C, is a transition from a crystal structure with dominant ionic chemical bonds to one with dominant covalent or covalent-metallic bonds.

The addition of ZrO_2 or HfO_2 into such substances in the concentration area of the H phase primary crystallization leads to an additional volume increase due to the appearance of chemically induced vacancies in the metal sublattice.

References

1. Frolov AA, Frolov YA, Andrievskaya ER, Kornienko OA. Possibilities of crystallization peculiarities in the focal zone of optical furnace used for melt density estimation. In: *Proc. int. conf.: modern material science: achievements and problems MMS–2005*. 2005. p. 834–5.
2. Frolov AA, Andrievskaya ER, Kornienko OA, Frolov YA. Crystallization peculiarities of the refractory alloys based on zirconia, yttria and erbia. *Refract Ind Ceram* 2007;**48**(3):1083–4877.
3. Mallet R. On the alleged expansion in volume of various substances in passing by refrigeration from the state of liquid fusion to that of solidification. *Proc R Soc Lond* 1874–1875;**23**:209–34.
4. Thomas MT, Ken AD. Predicting water's phase diagram and liquid-state anomalies. *J Chem Phys* 2002;**117**(11):5101–4.
5. Tanaka H. Thermodynamic anomaly and polymorphism of water. *Europhys Lett* 2000;**50**(3):340–6.
6. Livshiz BG, Kraposhin VS, Linetzky YL. *Physical properties of metals and alloys*. Moscow: Metallurgiy; 1980 [in Russian].
7. Glazov VM, Chizhevskaya SN, Glagoleva NN. *Liquid semiconductors*. New York: Plenum Press; 1969.
8. Radchenko IV. Structure of liquid metals. *Adv Phys Sci* 1957;**61**(2):249–76 [in Russian].
9. Glazov VM, Schelicov OD. Temperature dependence of specific volume of the silicon and germanium near phase transitions of crystal–melt. *J Phys Chem* 2000;**74**(7):1258–65.
10. Sahara R, Mizuseki H, Ohno K, Uda S, Fukuda T, Kawazoe Y. Body-centered-cubic lattice model with many-body interactions representing the melting transition in Si. *J Chem Phys* 1999;**110**(19):9608–17.
11. Ivanova RV. *Chemistry and technology of gallium*. Moscow: Metallurgiy; 1973 [in Russian].
12. Hecker SS. Plutonium and its alloys. From atoms to microstructure. *Los Alamos Sci* 2000;**26**:290–335.
13. Basin AS, Kolotov YL, Vashukov IA. The density alteration of grey iron under slow crystallization. *Izvestiya AN SSSR Met* 1978;**3**:71–5 [in Russian].
14. Clark DL. The chemical complexities of plutonium. *Los Alamos Sci* 2000;**26**:364–81.
15. Tanaka H. Simple view of waterlike anomalies of atomic liquids with directional bonding. *Phys Rev B* 2002;**66**:064202.
16. Pauling L. *General chemistry*. San-Francisco: W.H. Freeman and Company; 1970.
17. Savitskiĭ EM, Terekhova VF, Naumkin OP. Physico-chemical properties of the rare-earth metals, scandium, and yttrium. *Sov Phys Uspekhi* 1963;**6**(1):123–42.
18. Pfann WG. *Zone melting*. New York, London, Sydney: John Wiley & Sons, Inc.; 1966.
19. Bradshaw SE. *J Electrochem Soc* 1957;**101**(6):293–7.
20. Frolov AA, Frolov YA. Quantitative estimation problems of material crystallization volume effect under the influence of centre radial symmetry heating. In: *Proc. of the fourth int. conf. MEE-2006 "Materials and Coatings for Extreme Performances: Investigations, Applications, Ecologically Safe Technologies for Their Production and Utilization"*. 2006.
21. Frolov AA, Andrievskaya ER. Abnormal crystallization of some alloys in the system ZrO_2–Y_2O_3–Er_2O_3. In: *Proc. of the fourth int. conf. MEE–2006 "Materials and Coatings for Extreme Performances: Investigations, Applications, Ecologically Safe Technologies for Their Production and Utilization"*. 2006.
22. Frolov AA, Voynich EV, Garbuz VV. Peculiarities of crystallization of alumina, yttria and rare-earth element oxides of yttria subgroup in an optical furnace. *J Eur Ceram Soc* 2010, doi:10.1016/j.jeurceramsoc.2010.04.002.
23. Frolov A, Frolov Yu, Andrievskaya E. Anomalous crystallization of some alloys in refractory oxide systems based on zirconia, yttria and erbia. *High Temperature Mater Process* 2007;**26**(3):221–9.
24. Frolov AA, Voinich EV, Frolov YuA. Method for evaluating the change in specific volume of refractory substances during crystallization. *Refract Ind Ceram* 2008;**49**(3):183–8.
25. Lopato LM, Shevchenco AV, Nigmanov AV. Y_2O_3–Er_2O_3 system. *Izv AS USSR Inorg Mater* 1984;**20**(3):446–8 [in Russian].
26. Arsenyev PA, Kovba LM, Bagdasarov KhS, Dzhurinskii BF, Potemkin AV, Pokrovskii BI, et al. *Compounds of rare-earth elements: systems with the oxides of elements from groups I–III*. Moscow: Nauka; 1983 [in Russian].
27. Ormont BF. *Introduction to semiconductor physical chemistry and crystallochemistry*. Moscow: Vysshaya Shkola; 1963 [in Russian].
28. Andrievskaya ER, Lopato LM, Shevchenco AV. Liquidus surface of the phase diagram ZrO_2–Y_2O_3–Er_2O_3 system. *Izv RAN Neorgan Mater* 1996;**32**(6):721–6 [in Russian].
29. Pascual C, Duran P. Phase equilibria and ordering in the erbia–zirconia system. *J Mater Sci* 1981;**16**(11):3067–76.
30. Trubelia MF, Stubican VS. Phase equilibria and ordering in the system zirconia–hafnia–yttria. *J Am Ceram Soc* 1988;**71**(8):662–6.